




## ORIGINAL ARTICLE

# ELOVL5-mediated fatty acid elongation promotes cellular proliferation and invasion in renal cell carcinoma

Satoshi Nitta<sup>1</sup>  | Shuya Kandori<sup>1</sup>  | Ken Tanaka<sup>2</sup> | Shotaro Sakka<sup>1</sup> | Masanobu Siga<sup>1</sup> | Yoshiyuki Nagumo<sup>1</sup> | Hiromitsu Negoro<sup>1</sup> | Takahiro Kojima<sup>3</sup> | Bryan J. Mathis<sup>4</sup> | Toru Shimazui<sup>5</sup> | Takafumi Miyamoto<sup>6</sup> | Takashi Matsuzaka<sup>6</sup> | Hitoshi Shimano<sup>6</sup> | Hiroyuki Nishiyama<sup>1</sup> 

<sup>1</sup>Department of Urology, Faculty of Medicine, University of Tsukuba, Tsukuba, Japan

<sup>2</sup>Department of Urology, Tsukuba Medical Center Hospital, Tsukuba, Japan

<sup>3</sup>Department of Urology, Aichi Cancer Center Hospital, Nagoya, Japan

<sup>4</sup>International Medical Center, University of Tsukuba Affiliated Hospital, Tsukuba, Japan

<sup>5</sup>Department of Urology, Ibaraki Prefectural Central Hospital, Kasama, Japan

<sup>6</sup>Department of Endocrinology and Metabolism, Faculty of Medicine, University of Tsukuba, Tsukuba, Japan

## Correspondence

Shuya Kandori, Department of Urology, Faculty of Medicine and Graduate School of Comprehensive Human Science, University of Tsukuba, 1-1-1 Tennodai, Tsukuba, Ibaraki 305-8575, Japan.  
Email: [shuya79@md.tsukuba.ac.jp](mailto:shuya79@md.tsukuba.ac.jp)

## Funding information

This work was supported by a grant from the Japan Society for the Promotion of Science KAKENHI (no. 19K09664) and a grant from COI-NEXT (no. JPMJPF2017).

## Abstract

Renal cell carcinoma (RCC) features altered lipid metabolism and accumulated polyunsaturated fatty acids (PUFAs). Elongation of very long-chain fatty acid (ELOVL) family enzymes catalyze fatty acid elongation, and ELOVL5 is indispensable for PUFAs elongation, but its role in RCC progression remains unclear. Here, we show that higher levels of ELOVL5 correlate with poor RCC clinical prognosis. Liquid chromatography/electrospray ionization-tandem mass spectrometry analysis showed decreases in ELOVL5 end products (arachidonic acid and eicosapentaenoic acid) under CRISPR/Cas9-mediated knockout of ELOVL5 while supplementation with these fatty acids partially reversed the cellular proliferation and invasion effects of ELOVL5 knockout. Regarding cellular proliferation and invasion, CRISPR/Cas9-mediated knockout of ELOVL5 suppressed the formation of lipid droplets and induced apoptosis via endoplasmic reticulum stress while suppressing renal cancer cell proliferation and in vivo tumor growth. Furthermore, CRISPR/Cas9-mediated knockout of ELOVL5 inhibited AKT Ser473 phosphorylation and suppressed renal cancer cell invasion through chemokine (C-C motif) ligand-2 downregulation by AKT-mTOR-STAT3 signaling. Collectively, these results suggest that ELOVL5-mediated fatty acid elongation promotes not only cellular proliferation but also invasion in RCC.

## KEYWORDS

cellular invasion, cellular proliferation, elongation of very long-chain fatty acid 5, polyunsaturated fatty acid, renal cell carcinoma

**Abbreviations:** AA, arachidonic acid; ccRCC, clear cell renal cell carcinoma; chRCC, chromophobe renal cell carcinoma; DEG, differentially expressed gene; ELOVL, elongation of very long-chain fatty acid; EPA, eicosapentaenoic acid; ER, endoplasmic reticulum; FA, fatty acid; FBS, fetal bovine serum; FPKM, fragments per kilobase per million mapped reads; GDC, Genomic Data Commons; LC/ESI-MS/MS, liquid chromatography/electrospray ionization-tandem mass spectrometry; LC-FA, long-chain fatty acid; LD, lipid droplet; mTOR, mammalian target of rapamycin; OA, oleic acid; OS, overall survival; pRCC, papillary renal cell carcinoma; PUFA, polyunsaturated fatty acid; RCC, renal cell carcinoma; RPMI, Roswell Park Memorial Institute; SCD1, stearyl-CoA desaturase 1; TCGA, The Cancer Genome Atlas; UPR, unfolded protein response; VEGF, vascular endothelial growth factor.

This is an open access article under the terms of the [Creative Commons Attribution-NonCommercial-NoDerivs](https://creativecommons.org/licenses/by-nc-nd/4.0/) License, which permits use and distribution in any medium, provided the original work is properly cited, the use is non-commercial and no modifications or adaptations are made.

© 2022 The Authors. *Cancer Science* published by John Wiley & Sons Australia, Ltd on behalf of Japanese Cancer Association.

## 1 | INTRODUCTION

Fatty acids (FAs) comprising lipids, such as triglycerides, sphingo-lipids, and phospholipids, are important structural, energy, and signaling sources. FA length is a crucial functional indicator, and the rate-limiting steps of de novo long-chain fatty acid (LC-FA) synthesis are regulated by the conserved elongation of very long-chain fatty acid enzyme family (ELOVLs).<sup>1</sup> A total of seven ELOVLs are currently recognized and categorized into saturated and monounsaturated FA-specific (ELOVL1, ELOVL3, ELOVL6, and ELOVL7) and polyunsaturated fatty acid (PUFA)-specific activities (ELOVL2, ELOVL4, and ELOVL5).<sup>2</sup> Altered lipid metabolism is a key cancer biomarker because turnover is accelerated within the tumor microenvironment.<sup>2,3</sup>

Renal cell carcinoma (RCC), roughly 2% of total adult malignancies, is usually found as clear cell RCC (ccRCC), with papillary RCC (pRCC) and chromophobe RCC (chRCC) following.<sup>4</sup> If RCC is localized, partial or radical nephrectomy are usually curative,<sup>5,6</sup> while unresectable or metastatic RCC cases receive drugs targeting vascular endothelial growth factor (VEGF), immune checkpoints, and mammalian target of rapamycin (mTOR).<sup>4,5</sup> These therapies have somewhat improved prognoses, but outcomes remain dismal.<sup>5</sup>

ELOVL5 elongates linoleic acid (18:2, n-6) and  $\alpha$ -linolenic acid (18:3, n-3) to form arachidonic acid (AA, 20:4, n-6) and eicosapentaenoic acid (EPA, 20:5, n-3), respectively. Recent studies, including our own, indicate RCC as a metabolic disease in which expression and bioaccumulation of ELOVL2/ELOVL5 and PUFAs occur, while ELOVL2 suppresses cellular apoptosis and promotes cellular proliferation via regulation of lipid metabolism.<sup>7,8</sup> However, the significance of ELOVL5 in RCC remains unclear. Therefore, we explored the role of FA elongation, as regulated by ELOVL5, on RCC progression.

Here, we show that inhibition of ELOVL5 alters lipid metabolism and ablates cellular proliferation in favor of apoptosis, ostensibly from enhanced endoplasmic reticulum (ER) stress. Furthermore, we show that ELOVL5-mediated lipid metabolism is linked to AKT activation, which may contribute to cellular invasion. This is the first demonstration linking ELOVL5-mediated PUFA elongation and renal cancer progression.

## 2 | MATERIALS AND METHODS

### 2.1 | Patients and RCC samples

Tumor specimens from 40 patients who underwent either radical or partial nephrectomies were obtained from the University of Tsukuba Hospital under protocols approved by the Ethics Committee of the University of Tsukuba (approval number: H28-104). All patients gave written, informed consent. Tumor stages were assigned according to the TNM staging of the Union for International Cancer Control.<sup>9</sup> Pathological grades were classified by the Fuhrman grading system.<sup>10</sup>

### 2.2 | Immunohistochemistry

Immunohistochemistry was conducted as described previously.<sup>11</sup> Primary antibodies can be found in Table S1. The labeling index for Ki-67 was calculated as the percentage of positive tumor nuclei divided by the total number of tumor cells examined.

### 2.3 | Cell lines and cell cultures

ACHN and 786-O cell lines were purchased from ATCC, while the OS-RC-2 cell line was purchased from the RIKEN BioResource Center. The SKRC52 cell line was kindly gifted by Dr. L.J. Old (Ludwig Institute for Cancer Research). Human RPTEC cells from the renal proximal tubule epithelium were purchased from Colnetics. These cell lines were cultured in Roswell Park Memorial Institute (RPMI) 1640 medium with 10% fetal bovine serum (FBS) at 37°C with a 5% humidified CO<sub>2</sub> atmosphere. Cell lines transfected with CRISPR/Cas9-mediated knockout of ELOVL5 were cultured in the presence of G418.

### 2.4 | FA preparation

AA (Wako, Cat #194625) and EPA (Cayman Chemical, Cat #90110) were dissolved in ethanol and mixed vigorously to a final concentration of 10mM, filter-sterilized, and added to the culture medium with 0.5% FA-free BSA (Wako, Cat #017-15141) in phosphate-buffered saline to 10 $\mu$ M final concentration.

### 2.5 | Western blot analysis

Western blot analysis was performed as described previously.<sup>8,12</sup> The primary antibodies used are listed in Table S1.  $\beta$ -actin was used as an internal control.

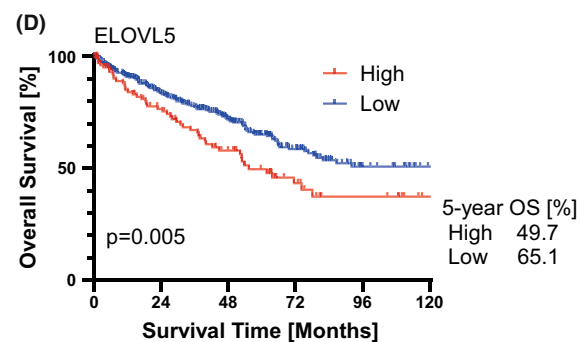
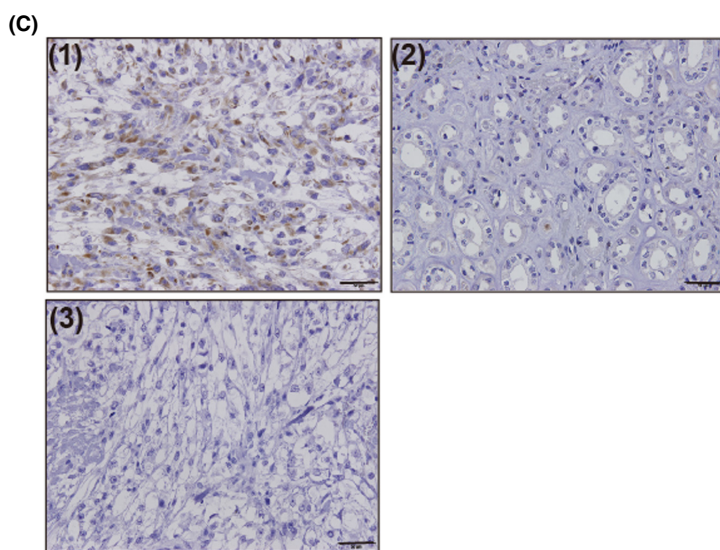
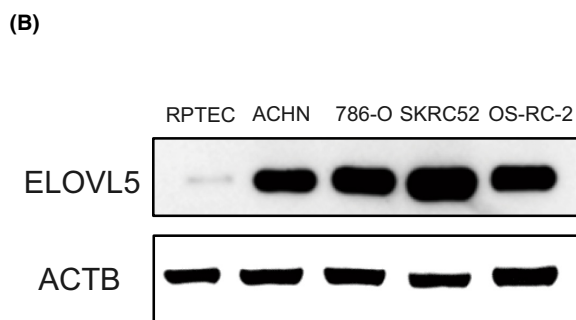
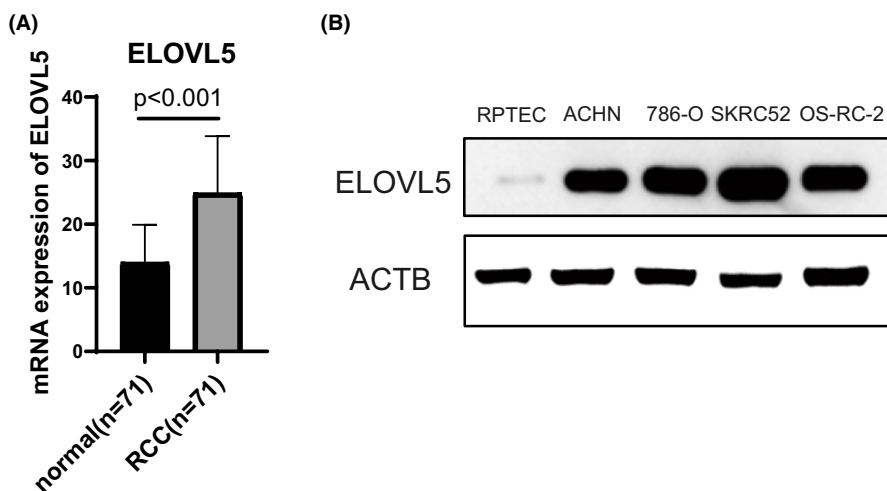
### 2.6 | CRISPR/Cas9-mediated knockout of ELOVL5

The pX330-U6-Chimeric\_BB-CBh-hSpCas9 (pX330) plasmid was generously gifted by Feng Zhang (Addgene plasmid # 42230).<sup>13</sup> The CRISPR single-guide RNAs (sgRNAs) for ELOVL5 were designed using the online tool CRISPR Design Tool (Dharmacon, <http://dharmacon.horizondiscovery.com/gene-editing/crispr-cas9/crispr-design-tool/>) before cloning into the pX330 plasmid, and these sequences are shown in Table S2. The CRISPR sgRNA for control (sgControl) was previously designed.<sup>14</sup> We transfected ACHN and 786-O cells with the CRISPR/Cas9 ELOVL5 oligos and selected for positive clones by G418. After transfection, single cells were cloned in 96-well plates via limiting dilution method. Transfected strains derived from a single clone were cultured before knockout of ELOVL5 was verified by Western blot analysis.

## 2.7 | Nude mouse xenograft assays

Female 6 to 8-week-old Balb/c nude (nu/nu) mice were purchased from Charles River Laboratories Japan. For subcutaneous xenograft assays,  $1 \times 10^7$  cells were injected subcutaneously into the flank. Orthotopic xenografts were performed as described previously.<sup>15</sup> Briefly, a 2-cm incision was made on the left flank to expose the

kidney before  $1 \times 10^6$  cells were injected into the renal parenchyma. Mice were sacrificed at 12 weeks after injection. Tumor masses were confirmed by hematoxylin and eosin staining. All experiments involving laboratory animals were performed in accordance with the Guideline for Animal Experiments of the University of Tsukuba. All experiments were approved by the Institutional Animal Care and Use Committee, University of Tsukuba (approval number: 21-361).



		No. at risk					
High	Low	110	69	40	18	9	2
High	Low	420	275	160	71	27	12

**FIGURE 1** ELOVL5 is overexpressed in renal cell carcinoma (RCC), and this overexpression is associated with poor prognosis in RCC patients. A, The mRNA expression of ELOVL5 in corresponding normal and tumor tissues as reported by The Cancer Genome Atlas (TCGA) data ( $N = 71$ ). Statistical analysis was performed by Student's *t* test. B, Western blot analysis of ELOVL5 in RCC cell lines (ACHN, 786-O, SKRC52, and OS-RC-2) and normal renal proximal tubule cell line (RPTEC). C, Representative images of ELOVL5 immunohistochemical staining. (1) Primary tumor. (2) Corresponding normal tissue. (3) Negative control of primary tumor in (1) stained with a control antibody (rabbit IgG). Scale bar, 50  $\mu$ m. D, Kaplan-Meier curves of the overall survival (OS) of 530 ccRCC patients in the TCGA dataset. Statistical analysis was performed by log-rank test

## 2.8 | Bioinformatics analysis of gene expression

Clinical and RNA sequencing data of 530 primary tumors and 72 control samples collected from RCC patients (KIRC) in The Cancer Genome Atlas (TCGA) database were downloaded from the Genomic Data Commons (GDC) Data Portal.<sup>16</sup> The mRNA expression level was measured as fragments per kilobase per million mapped reads (FPKM). To compare mRNA expression of ELOVL5 in corresponding normal and tumor tissues, we excluded one control sample without available data from a corresponding primary tumor. For survival analysis, 530 patients were divided into two groups (low and high expression) using expression cutoff values that yielded maximal survival differences between groups at the lowest log-rank *P* value.

## 2.9 | Liquid chromatography/electrospray ionization-tandem mass spectrometry (LC/ESI-MS/MS) analysis of FA metabolites

Fatty acid metabolites were purified from lipid fractions by solid-phase extraction with Oasis HLB columns (Waters Corporation). Purification and liquid chromatography were performed as described previously.<sup>17,18</sup> Briefly, FA metabolites were extracted from  $4 \times 10^7$  cells with internal standards. FA metabolites were then separated using a high-performance liquid chromatography system (Nexera LC-30AD, Shimadzu Corporation) equipped with an XBridge C18 column (particle size 3.5  $\mu$ m, length 150 mm, inner diameter 1.0 mm; Waters) and analyzed on a triple quadrupole mass spectrometer (LCMS-8040; Shimadzu). Mass spectrometry analyses were carried out in negative ion mode while FA metabolites were analyzed via multiple reaction monitoring, as previously reported.<sup>17,18</sup> For quantification, calibration curves were prepared for each compound and deuterated internal standards were used to monitor recoveries. Data analysis was performed with LabSolutions software (Shimadzu Corporation).

## 2.10 | Statistical analysis

Data were expressed as mean  $\pm$  SD, except for subcutaneous xenograft assays (mean  $\pm$  SE). Categorical variables were compared between cohorts using Pearson's chi-squared test for two or more variables. Continuous variables were compared using the Student *t* and Wilcoxon rank sum tests. Calculation of survival data was performed according to the Kaplan-Meier method and compared between groups by the log-rank test. To check for correlations between two variables, a Spearman correlation (*r*) and statistical significance of *r* were calculated. *P* values  $< 0.05$  were considered statistically significant. GraphPad Prism8 (GraphPad Software) and SPSS® 25.0 for Windows® (SPSS Inc.) were used for the statistical analyses.

Additional materials and methods are detailed in [Data S1](#). Our RNA-sequencing data are available at GSE192403.

## 3 | RESULTS

### 3.1 | ELOVL5 is overexpressed in RCC and higher levels of ELOVL5 expression correlate with poor clinical prognoses in RCC patients

We confirmed significant elevation of ELOVL5 mRNA and protein expression levels in RCC compared with control tissue (Figure 1A–C). In immunohistochemical analysis, 30 of 40 ccRCC cases showed significantly higher clinical staging coupled to higher ELOVL5 staining intensities (Table 1). Patient characteristics and ELOVL5 staining statuses are summarized in Table 1.

Next, we explored the tumor progression role of ELOVL5 in RCC patients using TCGA database (KIRC cohort). As shown in Figure 1D, overall survival (OS) was negatively associated with increased ELOVL5 expression, linking ELOVL5 and RCC disease progression.

### 3.2 | CRISPR/Cas9-mediated knockout of ELOVL5 reduces RCC proliferation and invasion ability

To examine whether ELOVL5 regulates proliferative and invasive ability, we knocked out ELOVL5 expression with two independent CRISPR/Cas9 sgRNAs (#1 and #2), both of which markedly reduced ELOVL5 protein levels in ACHN and 786-O cells (Figure 2A). We then performed WST-8 and Matrigel invasion assays to detail any effects of CRISPR/Cas9-mediated knockout of ELOVL5 in renal cancer cells. As shown in Figure 2B,C, CRISPR/Cas9-mediated knockout of ELOVL5 significantly suppressed the cellular proliferation and invasion of both cell lines in vitro, suggesting a key role for ELOVL5 in mediating such activities in renal cancer cells.

TABLE 1 Characteristics of 40 patients with clear cell renal cell carcinoma (ccRCC) at the University of Tsukuba Hospital

	ccRCC (N = 40)		<i>p</i>
	High ELOVL5 <sup>a</sup> (N = 30)	Low ELOVL5 <sup>a</sup> (N = 10)	
Age (mean $\pm$ SD)	67.9 $\pm$ 12.7	63.2 $\pm$ 10.4	0.298
Clinical stage			
Stage 1/2	12	8	0.029
Stage 3/4	18	2	
Pathological T stage			
T1/2	14	8	0.067
T3/4	16	2	
Grade			
G1-2	15	7	0.271
G3-4	15	3	

<sup>a</sup>Staining intensity compared with corresponding normal tissue.

### 3.3 | CRISPR/Cas9-mediated knockout of ELOVL5 reduces tumor growth and invasion in vivo

We used a nude mouse xenograft model to examine the tumor progression role of ELOVL5 in RCC, finding that CRISPR/Cas9-mediated knockout of ELOVL5 in ACHN and 786-O cell lines suppressed tumor growth after subcutaneous implantation (Figure 3A). We next calculated the Ki-67 index in xenograft tumors infected with sgControl or sgELOVL5 and found significant differences among tumors in the two groups (Figure 3B). Furthermore, we performed orthotopic xenograft assays in ACHN cell lines to examine whether ELOVL5 regulates renal cancer cell invasion in vivo. As shown in Figure 3C, sgControl cells infiltrated into normal kidney parenchyma whereas sgELOVL5 cells stopped

well before. These results further support the capacity of ELOVL5 in RCC proliferative and invasive abilities.

### 3.4 | ELOVL5 elongation of polyunsaturated FAs is critical for cellular proliferation of and invasion by RCC

To examine the alteration of lipid metabolism under CRISPR/Cas9-mediated knockout of ELOVL5, we examined total FA levels between ACHN/sgControl and ACHN/sgELOVL5 cells by LC/ESI-MS/MS analysis. As expected, AA and EPA levels were reduced in sgELOVL5 cells compared with sgControl cells (Figure 4A) and, furthermore, we found that AA or EPA supplementation partially reversed the

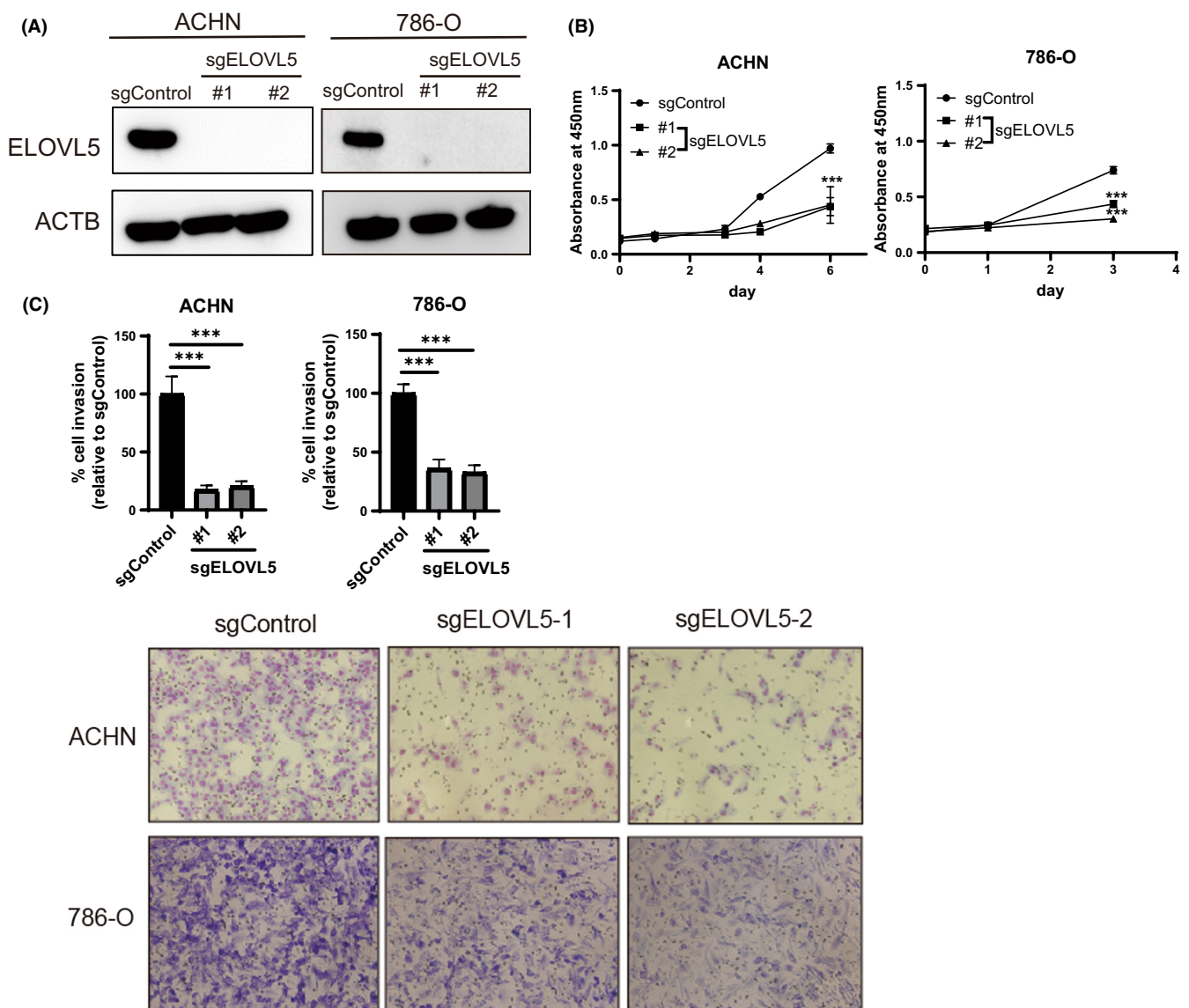


**FIGURE 2** CRISPR/Cas9-mediated knockout of ELOVL5 suppresses cellular proliferation and invasion in renal cell carcinoma (RCC) cell lines in vitro. A, Western blot analysis of ACHN and 786-O transfected with control or ELOVL5 sgRNA (#1, #2). B, Analysis of cell proliferation by WST-8 assay. C, Analysis of cell invasion by Matrigel invasion assay. Statistical analysis was performed by Student's *t* test (\* $p < 0.05$ , \*\* $p < 0.01$ , \*\*\* $p < 0.001$ )



inhibitory effect of ELOVL5 knockout on cellular proliferation and invasion in both ACHN and 786-O cell lines (Figure 4B,C). These results indicate that ELOVL5-mediated PUFA elongation is crucial for cellular proliferation and invasion by RCC.

### 3.5 | CRISPR/Cas9-mediated knockout of ELOVL5 inhibits lipid droplet (LD) formation and induces the unfolded protein response (UPR)

As a clear biomarker of ccRCC is intracellular LDs that are related to disease progression,<sup>19-21</sup> we examined whether ELOVL5 promotes LD formation by live-cell staining with Lipi-Green probe. As shown in Figure 5A,B, the abundance of LDs in sgELOVL5 cells was significantly decreased compared with sgControl cells in ACHN and 786-O cell lines, while AA or EPA supplementation promoted LD formation

in both cell lines. Previous studies have shown that PUFAs (including AA and EPA) promote the formation of LDs,<sup>22,23</sup> in line with our results.

LD functions to protect against ER stress, maintain ER homeostasis, and control protein quality.<sup>19,20,24</sup> As decreased LD disrupts ER homeostasis, inducing the UPR and cell death,<sup>24</sup> we next examined the expression of UPR sensor proteins and target genes. As shown in Figure 5C, the phosphorylation of UPR sensor proteins PERK and IRE-1, as well as ATF6 expression, were increased in sgELOVL5 cells of both cell lines. Furthermore, the UPR target gene CHOP was increased in sgELOVL5 cells of both cell lines (Figure 5D,E). We next examined whether PUFAs affect the expression of CHOP and observed that AA or EPA supplementation partially reversed its expression (Figure 5F). These results suggest that ELOVL5-mediated lipid metabolism maintains ER homeostasis through LD formation to promote cellular proliferation.

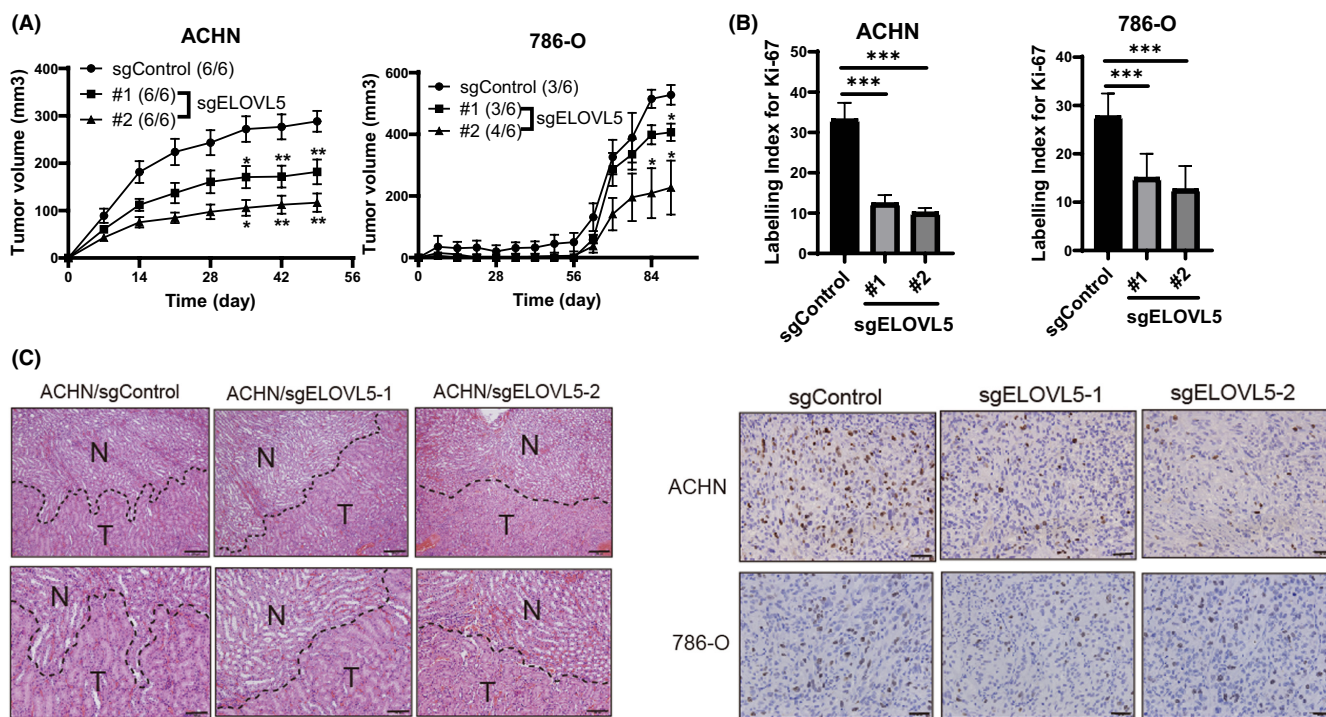
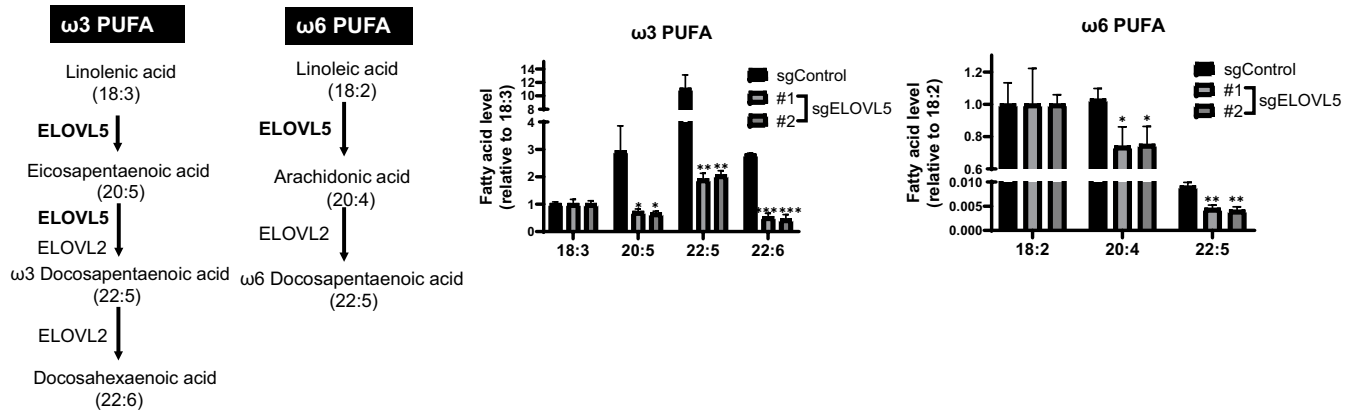


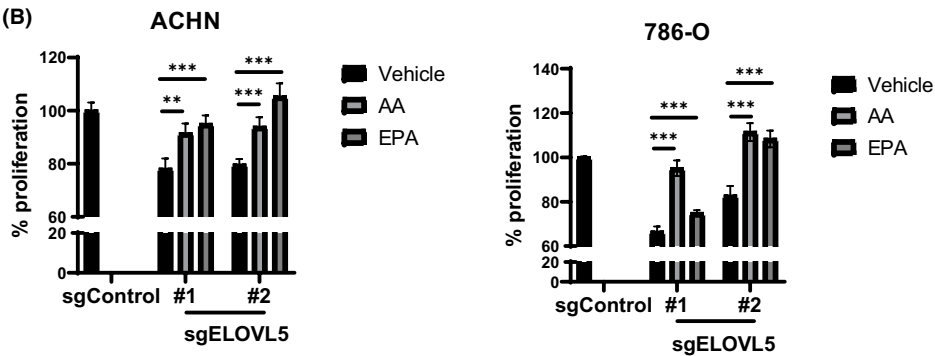
**FIGURE 3** CRISPR/Cas9-mediated knockout of ELOVL5 suppresses tumor growth and invasion in renal cell carcinoma (RCC) cell lines in vivo. A, The sequential changes of subcutaneous xenograft tumors from ACHN or 786-O cells transfected with control or ELOVL5 sgRNA. The numbers in parentheses indicate the number of animals developing tumors/total number of animals injected in each group. Statistical analysis was performed by Student's *t* test ( $*p < 0.05$ ,  $**p < 0.01$ ). The error bars represent the SE. B, Ki-67 staining of xenograft tumors developed from ACHN or 786-O cells transfected with control or ELOVL5 sgRNA. The labeling index for Ki-67 in xenograft tumor developed from ACHN or 786-O subclones are also shown. Statistical analysis was performed by Wilcoxon rank sum test ( $***p < 0.001$ ). Scale bar, 50 μm. C, Orthotopic implantation of ACHN cells transfected with control or ELOVL5 sgRNA. Upper panel: low-magnification view. Scale bar, 100 μm. Lower panel: high-magnification view. Scale bar, 200 μm. Tumor margins are indicated by dotted line. N, normal kidney tissue; T, tumor

**FIGURE 4** ELOVL5-mediated lipid metabolism is required for cellular proliferation and invasion in renal cell carcinoma (RCC). A, The measurement of polyunsaturated fatty acid (PUFA) by liquid chromatography/electrospray ionization-tandem mass spectrometry (LC/ESI-MS/MS) in ACHN/sgControl or ACHN/sgELOVL5 cells. B, Cellular proliferation rescue experiments with 10 μM arachidonic acid (AA, 20:4, n-6) or eicosapentaenoic acid (EPA, 20:5, n-3) after ELOVL5 knockout. C, Cellular invasion rescue experiments after ELOVL5 knockout. ACHN or 786-O cells were pretreated with 10 μM AA or EPA for 48 h before seeding into each well of the upper Matrigel invasion chamber. Statistical analysis was performed by Student's *t* test ( $*p < 0.05$ ,  $**p < 0.01$ ,  $***p < 0.001$ )

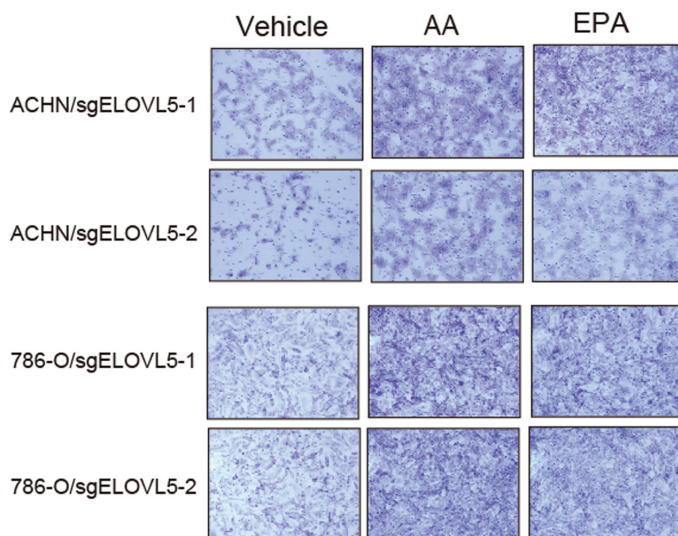
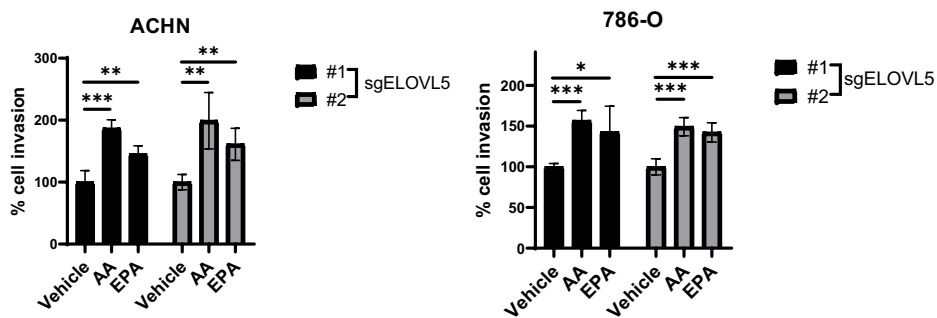
(A)



(B)



(C)



### 3.6 | CRISPR/Cas9-mediated knockout of ELOVL5 promotes ER stress-induced apoptosis

CHOP plays crucial roles in ER stress-induced apoptosis.<sup>25-27</sup> We examined whether apoptosis was induced in sgELOVL5 cells and

found that the activity of caspases 3 and 7 were significantly elevated in sgELOVL5-treated ACHN and 786-O cell lines (Figure 6A). As depolarized mitochondrial membrane potential is a crucial early-stage checkpoint in apoptosis,<sup>28</sup> we assessed such changes using a JC-1 assay that disassociates into monomers under membrane

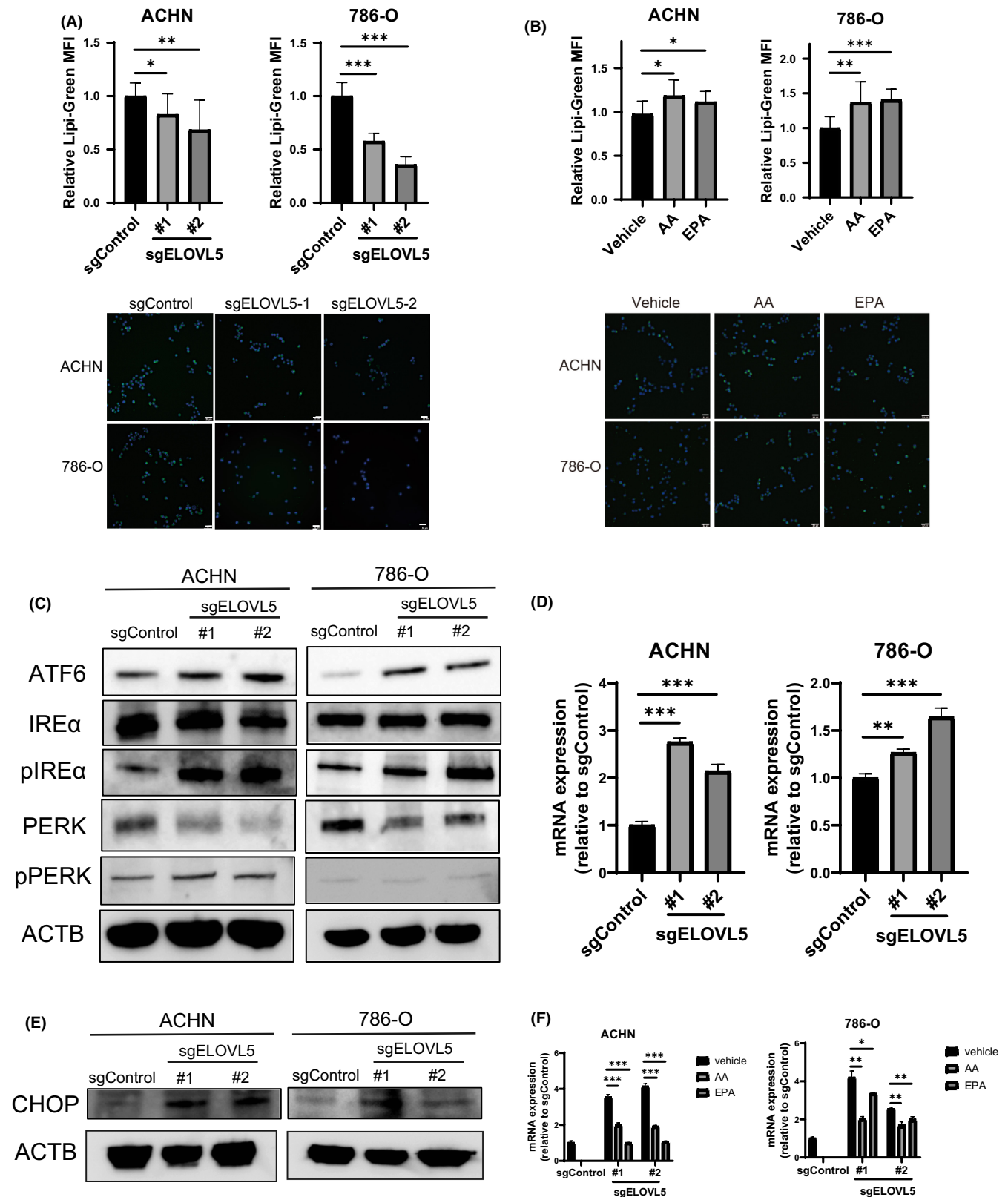




**FIGURE 5** CRISPR/Cas9-mediated knockout of ELOVL5 inhibits the formation of lipid droplets (LDs) and promotes the unfolded protein response. **A**, Representative images and quantification of LDs fluorescence in sgControl- or sgELOVL5-treated cells from ACHN and 786-O cell lines. **B**, Representative images and quantification of LD fluorescence in ACHN and 786-O cell lines treated with 10  $\mu$ M arachidonic acid (AA) or eicosapentaenoic acid (EPA) in 10% fatty acid-free, FBS-supplemented medium for 24 h. The same blank medium was used as a control (vehicle). Green: Lipi-Green. Blue: Hoechst33342. Scale bar, 50  $\mu$ m. **C**, Western blot analysis of unfolded protein response sensor proteins in sgControl- and sgELOVL5-treated cells from ACHN and 786-O cell lines. **D**, **E**, Evaluation of the expression of CHOP in sgControl- and sgELOVL5-treated cells from ACHN and 786-O cell lines by qRT-PCR (**D**) and Western blot analysis (**E**). **F**, Supplementation of AA or EPA partially reversed the mRNA expression of CHOP. The sgControl- and sgELOVL5-treated cells from ACHN and 786-O cell lines were given 10  $\mu$ M AA or EPA in 1% FBS-supplemented medium for 24 h before RNA was collected for qRT-PCR analysis. Statistical analysis was performed by Student's *t* test (\* $p$  < 0.05, \*\* $p$  < 0.01, \*\*\* $p$  < 0.001)

depolarization. Significant aggregate/monomer ratio decreases were observed, and the expression of pro-apoptotic genes (BAD, BAX, BAK, PUMA, and NOXA) was significantly increased in the sgELOVL5 cells of both cell lines (Figure 6B,C). Furthermore, sgELOVL5 cell viability after treatment with caspase inhibitor z-VAD-fmk was partially reversed in both cell lines (Figure 6D). We next examined whether PUFAs affect the expression of apoptotic genes, and supplementation of AA or EPA partially reversed the expression of those genes (Figure 6E). These results suggest that downregulation of lipid metabolism by ELOVL5 knockout induces apoptosis in renal cancer cells, at least in part through ER homeostatic disruption.

### 3.7 | ELOVL5 promotes cellular invasion through CCL2 regulation

The molecular details of how ELOVL5 promotes cancer invasion have not been reported. To explore this, we performed a global transcriptomic analysis and compared gene expression between ACHN/sgControl and ACHN/sgELOVL5 cells. Hierarchical clustering of 5849 significantly expressed genes was conducted (Figure 7A) and volcano plots showed significant expression profiles of 1178 differentially expressed genes (DEGs) between ACHN/sgControl and ACHN/sgELOVL5-1 cells, while 197 DEGs were found between ACHN/sgControl and ACHN/sgELOVL5-2 cells (Figure 7B). Next,

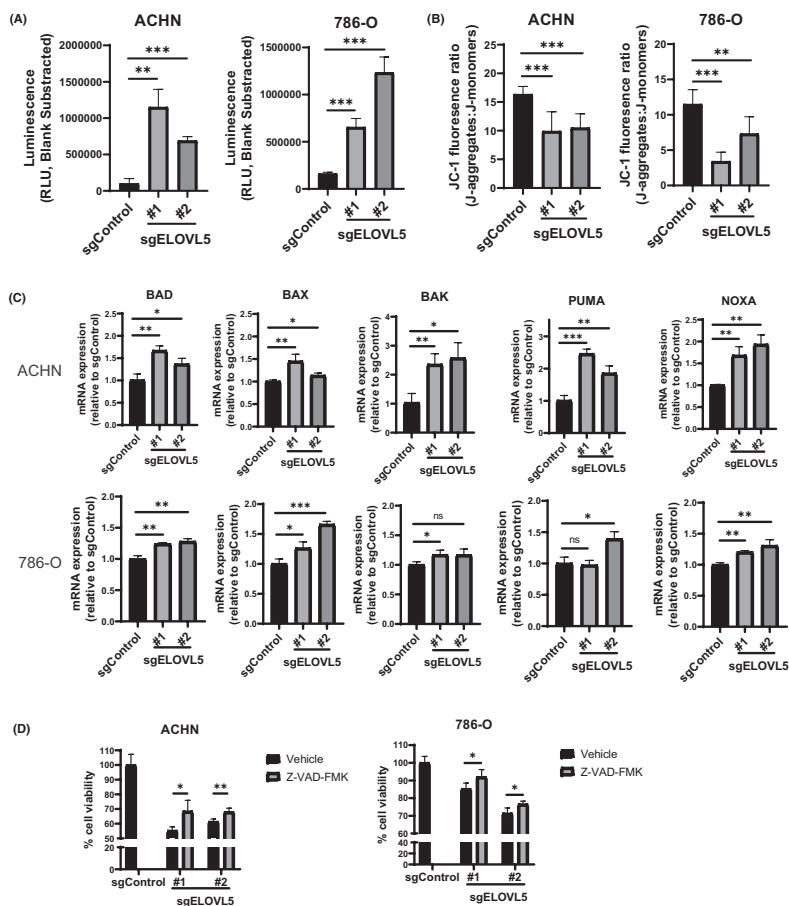


**FIGURE 6** (Continued)

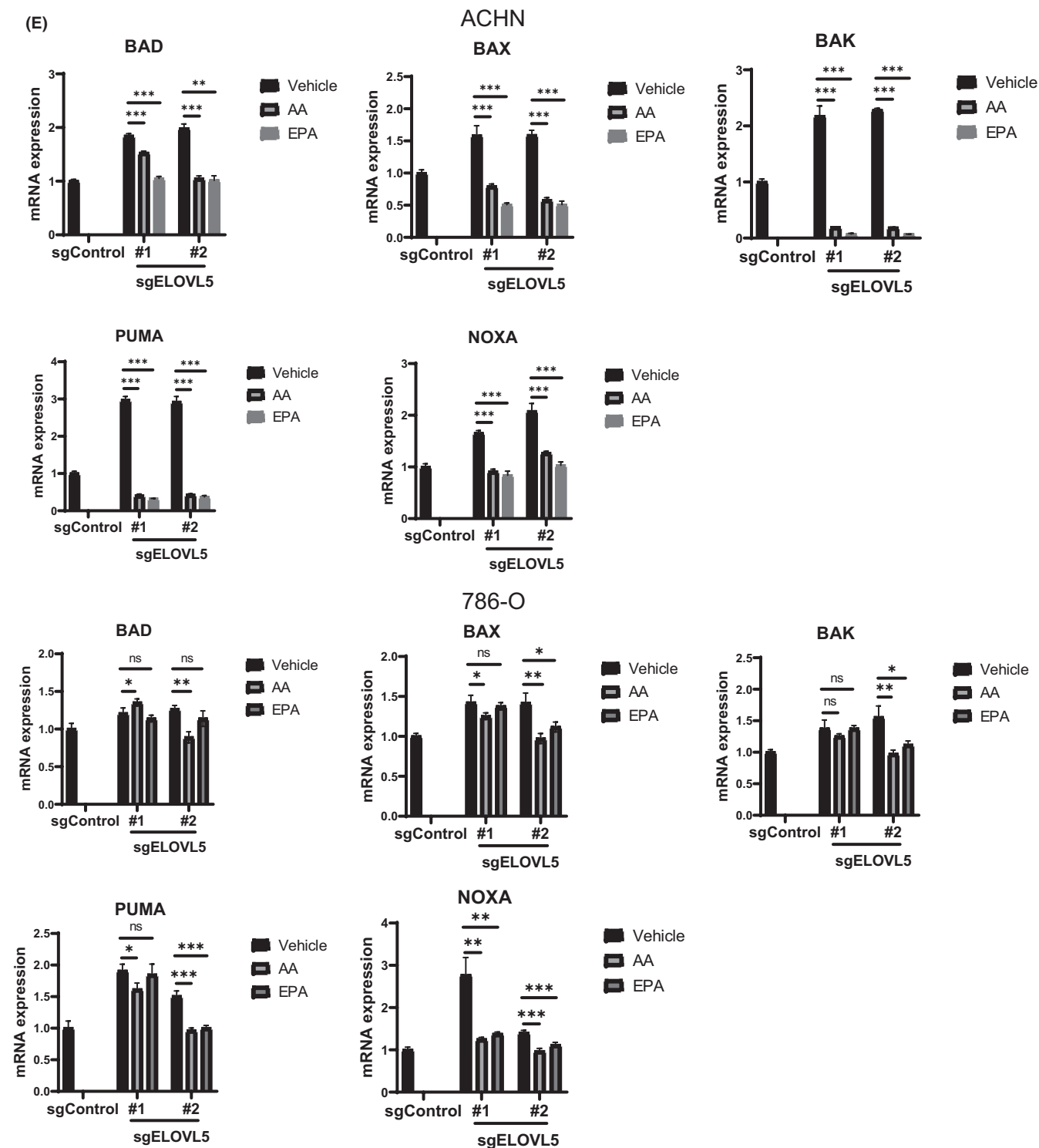


**FIGURE 6** CRISPR/Cas9-mediated knockout of ELOVL5 promotes apoptosis. A, B, Analysis of cell apoptosis by Caspase-3 and Caspase-7 assay (A) and JC-1 assay (B) in sgControl- and sgELOVL5-treated cells from ACHN and 786-O cell lines. C, The mRNA expression of pro-apoptotic genes was analyzed by qRT-PCR. D, Cell viability was measured by MTT assay in the presence or absence of 10  $\mu$ M z-VAD-FMK, a broad-spectrum caspase inhibitor. E, Supplementation of arachidonic acid (AA) or eicosapentaenoic acid (EPA) partially reverses the mRNA expression of pro-apoptotic genes. The sgControl- and sgELOVL5-treated cells from ACHN and 786-O cell lines were treated with 10  $\mu$ M AA or EPA in 1% FBS-supplemented medium for 24 h before RNA was collected for qRT-PCR analysis. The same blank medium was used as a control (vehicle). Statistical analysis was performed by Student's *t* test (\**p* < 0.05, \*\**p* < 0.01, \*\*\**p* < 0.001, ns, not significant)

we used ingenuity pathway analysis (IPA) to elucidate biological functions between the two groups using those DEGs, revealing a downregulation of cellular movement function in ACHN/sgELOVL5

cells compared with ACHN/sgControl cells (Figure 7C). After filtering of cellular movement-related genes by association with poor prognosis and positive correlation with ELOVL5 expression of 530

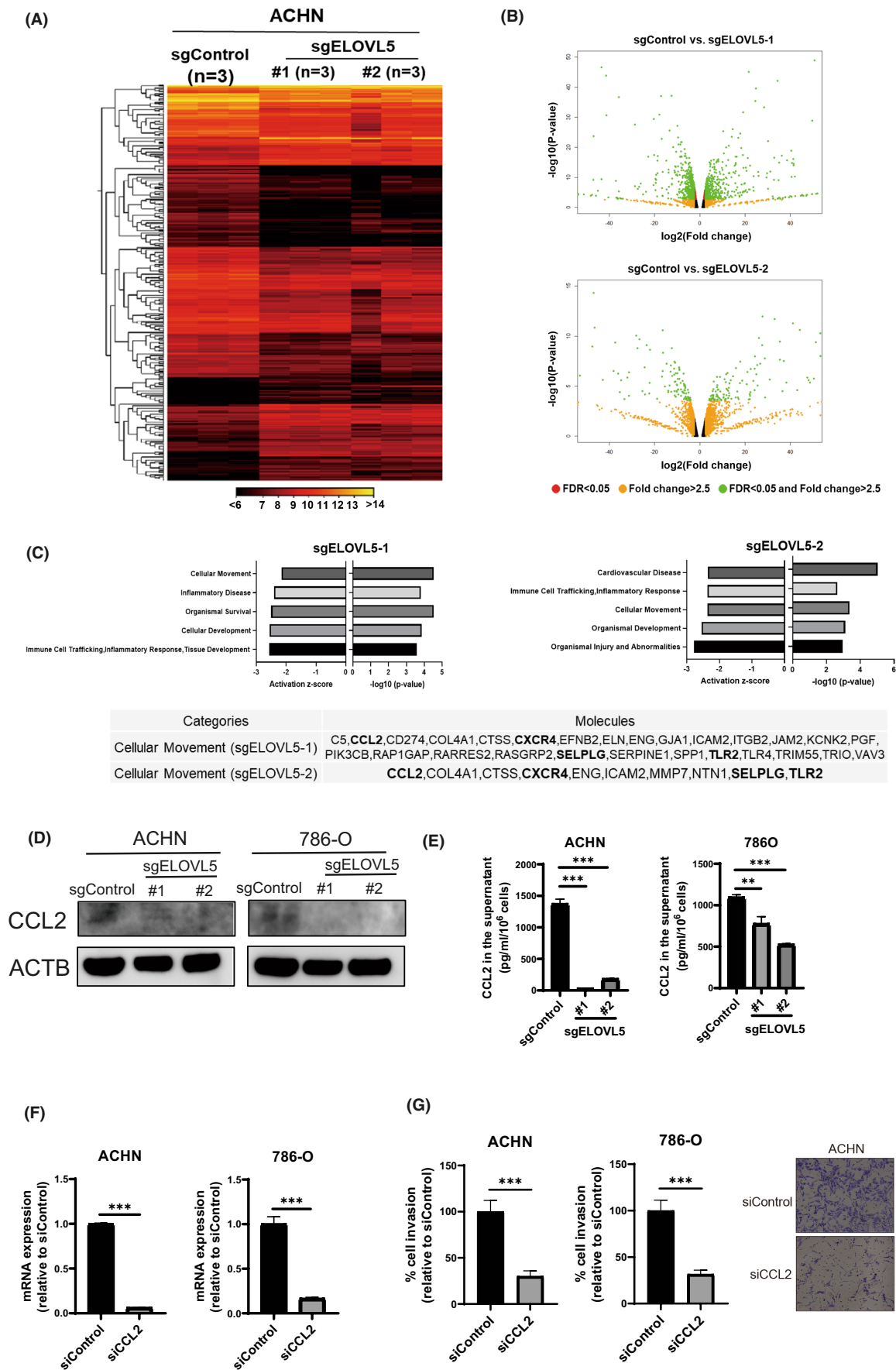


FIGURE 7 Legend on next page

**FIGURE 7** Global transcriptomic analysis using RNA sequencing showed that ELOVL5 associates with cellular movement via CCL2. A, Unsupervised clustering heatmap of ACHN/sgControl and ACHN/sgELOVL5 cells as generated by evaluating 5849 genes. B, A volcano plot showing differentially expressed genes (DEGs) distribution between ACHN/sgControl and ACHN/sgELOVL5 cells. DEGs are displayed in the indicated colors. C, The top five downregulated biological functions in ACHN/sgELOVL5 compared with those in ACHN/sgControl were analyzed by ingenuity pathway analysis (IPA). D, Western blot analysis of CCL2 in sgControl- and sgELOVL5-treated cells from ACHN and 786-O cell lines. E, CCL2 protein levels in the supernatants of sgControl- and sgELOVL5-treated cells from ACHN and 786-O cell lines were quantified using CCL2 ELISA kits. Concentration (pg/ml) was normalized to total cell. F, The mRNA expressions of CCL2 in ACHN and 786-O cells transfected with control or CCL2 siRNA were analyzed by qRT-PCR. G, Cellular invasion abilities of ACHN and 786-O cells transfected with control or CCL2 siRNA were analyzed by Matrigel invasion assay. Statistical analysis was performed by Student's *t* test. (\*\**p* < 0.01, \*\*\**p* < 0.001)

RCC patients in the TCGA dataset, we identified four genes: CCL2, CXCR4, SELPLG, and TLR2 (Table S3). Among these four genes, CCL2 was remarkably downregulated in both ACHN and 786-O cell lines (Figure S1), similar to previous reports that CCL2 promotes tumor migration and metastasis, and strengthening our assertion that CCL2 is a crucial cellular invasion gene associated with ELOVL5.<sup>29</sup>

The Cancer Genome Atlas data analysis revealed that increased CCL2 expression significantly correlated with poor prognosis, and this was also positively correlated with ELOVL5 expression (Figure S2A,B). Immunohistochemical analyses revealed that 29 of 40 ccRCC cases showed significantly higher CCL2 staining intensities (Figure S3) and 23 of 29 ccRCC cases (79.3%) were coupled to higher ELOVL5 staining intensities. The protein levels of CCL2 were significantly decreased in sgELOVL5 cells of both cell lines (Figure 7D,E). To firmly establish that CCL2 mediates cellular invasion by RCC cells, we next subjected ACHN and 786-O cells to CCL2-siRNA and observed significant decreases in CCL2 mRNA expression (Figure 7F). A Matrigel invasion assay using these same siRNA-treated cells resulted in significant suppression of cellular invasion by siRNA-treated cells of both cell lines (Figure 7G). Taken together, these results suggest that ELOVL5 promotes cellular invasion via CCL2 regulation.

### 3.8 | ELOVL5-mediated lipid metabolism promotes CCL2 upregulation through the phosphorylation of AKT Ser473 in RCC cells

To identify how ELOVL5 regulates CCL2 expression in RCC cells, we performed upstream regulator analysis using IPA in ACHN/sgControl and ACHN/sgELOVL5 cells. As shown in Figure 8A, AKT was identified as a potential kinase in ACHN cells. As AKT-mTOR-STAT3 signaling triggers CCL2 transcription,<sup>30-32</sup> we confirmed that the phosphorylation of AKT Ser473, mTOR Ser2448, and STAT3 Thr705 was significantly decreased by ELOVL5 ablation in ACHN and 786-O cell lines (Figure 8B). To further investigate this, we examined whether AA or EPA affects CCL2 expression and, as shown in Figure 8C, the mRNA expression of CCL2 was partially reversed with AA or EPA supplementation into the medium. Next, we examined whether AKT Ser473 phosphorylation is involved in altered lipid metabolism by ELOVL5 and saw a partial trend to increase after AA or EPA treatment (Figure 8D,E). Taken together, these results suggest that alteration of lipid metabolism by ELOVL5 promotes

renal cancer invasion through the upregulation of CCL2 by AKT-mTOR-STAT3 signaling.

## 4 | DISCUSSION

Here, we determined that ELOVL5 is essential in regulating RCC cancer progression. We established that it is overexpressed in RCC cells, and alteration of lipid metabolism by CRISPR/Cas9-mediated knockout of ELOVL5 affects the formation of LDs to ablate cellular proliferation through increased, ER stress-induced apoptosis. Furthermore, alteration of lipid metabolism by ELOVL5 knockout affects AKT-mTOR-STAT3 phosphorylation and transcription of CCL2, resulting in suppression of cellular invasion potential. These findings make ELOVL5 an attractive new therapeutic target.

As elongation and desaturation are integral to LC-FA production, previous studies focused on altered lipid metabolism in cancer and reported links between LC-FA and membrane formation, cell signaling, cell energetics, cellular proliferation, and metastasis. For example, in RCC, it was reported that ELOVL2 or Stearyl-CoA desaturase 1 (SCD1), part of the fatty acyl desaturase family, catalyzes the biosynthesis of monounsaturated fatty, oleic, and palmitoleic acids from the saturated FAs stearic and palmitic acid, promoting cellular proliferation.<sup>7,8,33</sup> While there are no reports demonstrating detailed mechanistic relationships between RCC and ELOVL5, ELOVL5 was reported as overexpressed in prostate cancer and oncogenic drug resistance.<sup>34,35</sup> Our paper adds mechanistic resolution to this scarce knowledge of cancer progression by ELOVL5 in the context of RCC.

We demonstrated that ELOVL5 knockout-mediated proliferation and invasion were partially rescued by AA or EPA supplementation (end products of the ELOVL5 pathway). AA is a pro-inflammatory precursor, and reports have demonstrated that AA pathway inhibition decreased cancer cell proliferation and invasion in several cancers, including RCC.<sup>36-39</sup> Conversely, EPA is an anti-inflammatory lipid mediator precursor and, while the anticancer effect of EPA was previously reported,<sup>36,40,41</sup> the detailed regulation of EPA metabolism in cancer remains unexplained. Our results conflict with previous reports, and a detailed EPA metabolic mechanism in RCC could not be fully elucidated in this study. However, clinically, Centenera et al showed that supplementation with PUFA in ELOVL5-depleted prostate cancer cells did not alter ELOVL5-mediated cell viability.<sup>35</sup> We assume that conflicting reports stem from the variable tumor



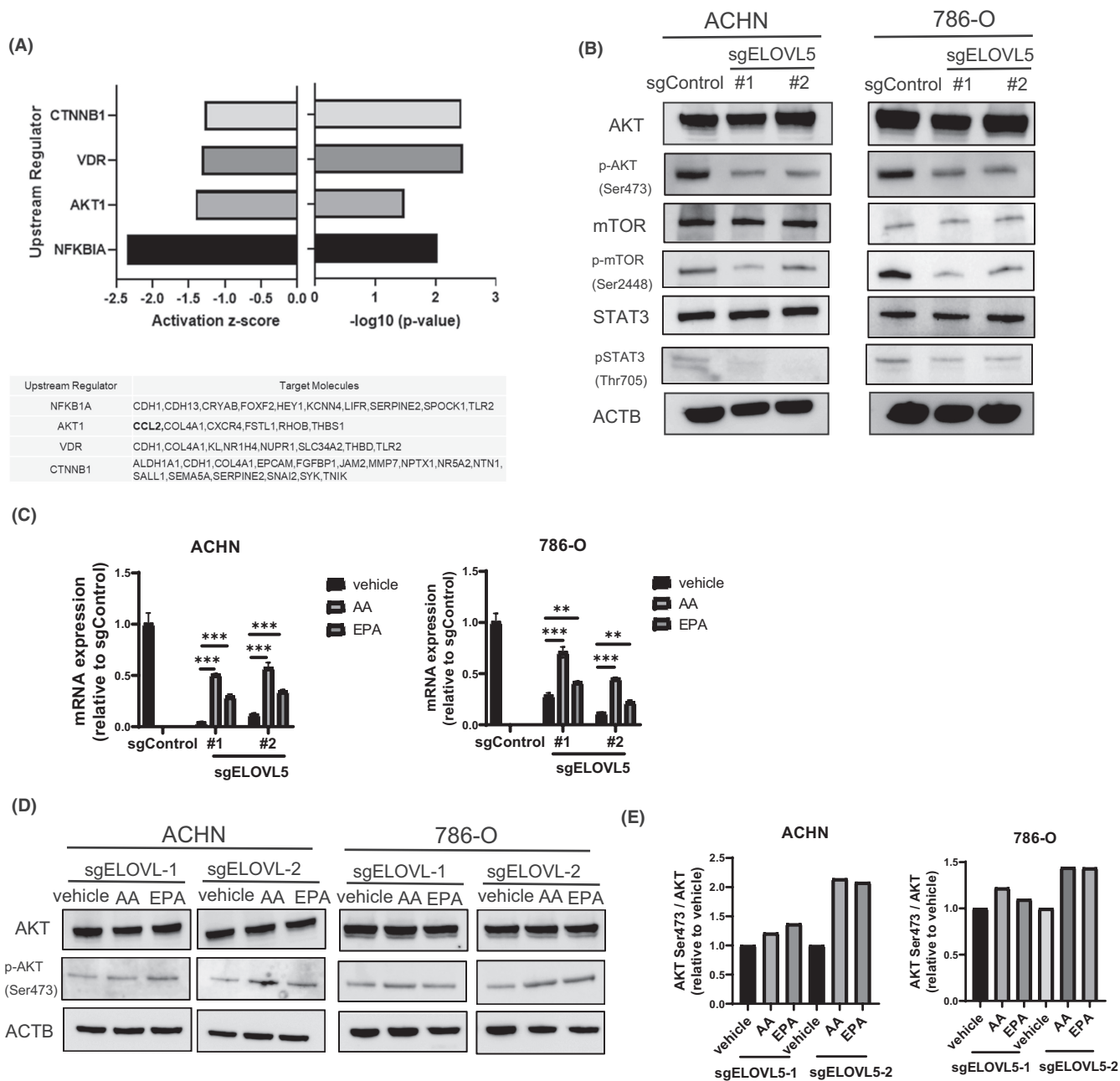


**FIGURE 8** ELOVL5-mediated lipid metabolism promotes CCL2 upregulation through the phosphorylation of AKT Ser473 in renal cell carcinoma (RCC) cells. **A**, Upstream regulator analysis was performed by ingenuity pathway analysis (IPA) in ACHN/sgControl and ACHN/sgELOVL5 cells. Results are shown as coexpression of ACHN/sgELOVL5-1 and ACHN/sgELOVL5-2. **B**, Western blot analysis of the phosphorylation levels of AKT Ser473, mTOR Ser2448, and STAT3 Thr705 in sgControl- and sgELOVL5-treated cells from ACHN and 786-O cell lines. **C**, Supplementation of arachidonic acid (AA) or eicosapentaenoic acid (EPA) partially reversed the reduced mRNA expression of CCL2. The sgControl- and sgELOVL5-treated cells from ACHN and 786-O cell lines were treated with 10  $\mu$ M AA or EPA in 1% FBS-supplemented medium for 24 h before RNA was collected for qRT-PCR analysis. **D**, Supplementation of AA or EPA partially reversed the reduced AKT phosphorylation in sgELOVL5-treated cells from ACHN and 786-O cell lines. ACHN and 786-O cell lines were treated with 10  $\mu$ M AA or EPA in 1% FBS-supplemented medium for 24 h before cell lysates were collected for Western blot analysis of AKT and AKT Ser473. The same blank medium was used as a control (vehicle). **E**, The ratio of AKT Ser473 and total AKT is shown. Bands were quantified using Image J software

microenvironment and that the homeostatic threshold of PUFAs required for cellular proliferation or invasion (via maintenance of membrane stability, energetics, etc.) may vary depending on tumor type. Future studies that profile tumor types from a PUFA standpoint

regarding EVOVL family activity will be instructive in highlighting therapeutic targets.

Lipid droplet accumulation is a cancer biomarker and functions as a complex effector, mediating proliferation, invasion, and

chemotherapy resistance in several cancers.<sup>20</sup> It has been reported that PUFAs promote LD formation,<sup>22,23</sup> and we demonstrated that CRISPR/Cas9-mediated knockout of ELOVL5 decreased AA and EPA levels while suppressing LD formation. LDs are also beneficial for ER homeostasis<sup>19,20</sup> because, under dysregulated ER stress, normal functions rapidly give way to apoptosis,<sup>42</sup> mediated in part by the CHOP pro-apoptotic transcription factor.<sup>42,43</sup> Our results showed that the mRNA expression of pro-apoptotic genes regulated by CHOP was increased by ELOVL5 knockout, leading to the conclusion that, collectively, ELOVL5 knockout inhibits LD formation and promotes ER stress-induced apoptosis.

Previous studies connected CCL2 with poor prognoses in patients with diverse cancers, including RCC.<sup>29,44,45</sup> The role of CCL2 in cancer is to stimulate cancer cell migration, activate vascular endothelial cells (resulting in angiogenesis), and recruit leukocytes.<sup>29</sup> We demonstrated that CCL2 is associated with cellular invasion in vitro and its expression is decreased by ELOVL5 knockout via ablation of AKT-mTOR-STAT3 signaling.<sup>30–32,46–48</sup> Phosphatidylinositol lipids (PI) are essential for phosphorylation of AKT, while acyl chain composition, as regulated by ELOVL5, mediates the biological activity of PI.<sup>49</sup> Regulation by endogenously synthesized FA on AKT activation is poorly understood but previous reports showed that the inhibition of SCD1 alters PI acyl chain composition from monounsaturated to more saturated acyl chains, resulting in an AKT phosphorylation decrease.<sup>50,51</sup> This was demonstrated by Rueda-Rincin et al and Xu et al who tied oleic acid (OA) and AA administration to increased AKT phosphorylation.<sup>34,51</sup> Our results are in line with these reports indicating that MUFA and PUFA are important FA in AKT phosphorylation. Future studies into direct binding assays will reveal any potential synergy between stearoyl-CoA desaturases and the ELOVL family of chain elongators.

In conclusion, this is the first demonstration linking ELOVL5-mediated PUFA elongation and renal cancer progression. Further analysis is necessary to elucidate the upstream role of ELOVL5 in the signaling pathway but our results suggest that ELOVL5 is a novel target molecule for suppressing RCC proliferation and invasion potential.

## ACKNOWLEDGMENTS

We are thankful for the skillful technical assistance of Mrs. Noriko Kunita and Mrs. Naoko Ueki (University of Tsukuba). We would like to thank LIPIDOME LAB Co., Ltd. for lipid analysis and Dr. Kazuhiro Yoshikawa (Aichi Medical University) for kindly providing the SKRC52 cell line.

## DISCLOSURE

The authors have no conflict of interest.

## ETHICAL APPROVAL

Approval of the research protocol by an Institutional Reviewer Board: Tumor specimens were obtained from the University of Tsukuba Hospital under protocols approved by the Ethics Committee of the University of Tsukuba (Approval Number: H28-104).

## INFORMED CONSENT

All patients gave written, informed consent.

## REGISTRY AND THE REGISTRATION NUMBER OF THE STUDY/TRIAL

n/a.

## ANIMAL STUDIES

All animal experiments were approved by the Institutional Animal Care and Use Committee, University of Tsukuba (Approval Number: 21-361).

## ORCID

Satoshi Nitta  <https://orcid.org/0000-0002-2855-1061>

Shuya Kandori  <https://orcid.org/0000-0003-4621-8470>

Hiroyuki Nishiyama  <https://orcid.org/0000-0001-7423-596X>

## REFERENCES

- Guillou H, Zdravec D, Martin PG, Jacobsson A. The key roles of elongases and desaturases in mammalian fatty acid metabolism: insights from transgenic mice. *Prog Lipid Res.* 2010;49(2):186-199.
- Koundouros N, Poulogiannis G. Reprogramming of fatty acid metabolism in cancer. *Br J Cancer.* 2020;122(1):4-22.
- Cheng C, Geng F, Cheng X, Guo D. Lipid metabolism reprogramming and its potential targets in cancer. *Cancer Commun.* 2018;38(1):27.
- Hsieh JJ, Purdue MP, Signoretti S, et al. Renal cell carcinoma. *Nat Rev Dis Primers.* 2017;3:17009.
- Choueiri TK, Motzer RJ. Systemic therapy for metastatic renal-cell carcinoma. *N Engl J Med.* 2017;376(4):354-366.
- Perazella MA, Dreicer R, Rosner MH. Renal cell carcinoma for the nephrologist. *Kidney Int.* 2018;94(3):471-483.
- Lucarelli G, Ferro M, Loizzo D, et al. Integration of Lipidomics and transcriptomics reveals reprogramming of the lipid metabolism and composition in clear cell renal cell carcinoma. *Metabolites.* 2020;10(12):509.
- Tanaka K, Kandori S, Sakka S, et al. ELOVL2 promotes cancer progression by inhibiting cell apoptosis in renal cell carcinoma. *Oncol Rep.* 2022;47(2):23.
- Paner GP, Stadler WM, Hansel DE, Montironi R, Lin DW, Amin MB. Updates in the eighth edition of the tumor-node-metastasis staging classification for urologic cancers. *Eur Urol.* 2018;73(4):560-569.
- Fuhrman SA, Lasky LC, Limas C. Prognostic significance of morphologic parameters in renal cell carcinoma. *Am J Surg Pathol.* 1982;6(7):655-663.
- Kandori S, Kojima T, Matsuoka T, et al. Phospholipase D2 promotes disease progression of renal cell carcinoma through the induction of angiogenin. *Cancer Sci.* 2018;109:1865-1875.
- Watanabe H, Hongu T, Yamazaki M, Kanaho Y. Phospholipase D2 activation by p38 MAP kinase is involved in neurite outgrowth. *Biochem Biophys Res Commun.* 2011;413(2):288-293.
- Cong L, Ran FA, Cox D, et al. Multiplex genome engineering using CRISPR/Cas systems. *Science.* 2013;339(6121):819-823.
- Miyamoto T, Lo PHY, Saichi N, et al. Argininosuccinate synthase 1 is an intrinsic Akt repressor transactivated by p53. *Sci Adv.* 2017;3(5):e1603204.
- Yang H, Minamishima YA, Yan Q, et al. pVHL acts as an adaptor to promote the inhibitory phosphorylation of the NF-kappaB agonist Card9 by CK2. *Mol Cell.* 2007;28(1):15-27.
- Grossman RL, Heath AP, Ferretti V, et al. Toward a shared vision for cancer genomic data. *N Engl J Med.* 2016;375(12):1109-1112.

17. Isobe Y, Arita M, Matsueda S, et al. Identification and structure determination of novel anti-inflammatory mediator resolvin E3, 17,18-dihydroxyeicosapentaenoic acid. *J Biol Chem.* 2012;287(13):10525-10534.
18. Hijioka M, Futokoro R, Ohto-Nakanishi T, Nakanishi H, Katsuki H, Kitamura Y. Microglia-released leukotriene B(4) promotes neutrophil infiltration and microglial activation following intracerebral hemorrhage. *Int Immunopharmacol.* 2020;85:106678.
19. Petan T, Jarc E, Jusović M. Lipid droplets in cancer: guardians of fat in a stressful world. *Molecules.* 2018;23(8):1941.
20. Li Z, Liu H, Luo X. Lipid droplet and its implication in cancer progression. *Am J Cancer Res.* 2020;10(12):4112-4122.
21. Qi X, Li Q, Che X, Wang Q, Wu G. The uniqueness of clear cell renal cell carcinoma: summary of the process and abnormality of glucose metabolism and lipid metabolism in ccRCC. *Front Oncol.* 2021;11:727778.
22. Guštin E, Jarc E, Kump A, Petan T. Lipid droplet formation in HeLa cervical cancer cells depends on cell density and the concentration of exogenous unsaturated fatty acids. *Acta Chim Slov.* 2017;64(3):549-554.
23. Yamamoto T, Takabatake Y, Minami S, et al. Eicosapentaenoic acid attenuates renal lipotoxicity by restoring autophagic flux. *Autophagy.* 2021;17(7):1700-1713.
24. Qiu B, Ackerman D, Sanchez DJ, et al. HIF2 $\alpha$ -dependent lipid storage promotes endoplasmic reticulum homeostasis in clear-cell renal cell carcinoma. *Cancer Discov.* 2015;5(6):652-667.
25. Malhotra JD, Miao H, Zhang K, et al. Antioxidants reduce endoplasmic reticulum stress and improve protein secretion. *Proc Natl Acad Sci USA.* 2008;105(47):18525-18530.
26. Marciniak SJ, Yun CY, Oyadomari S, et al. CHOP induces death by promoting protein synthesis and oxidation in the stressed endoplasmic reticulum. *Genes Dev.* 2004;18(24):3066-3077.
27. Song B, Scheuner D, Ron D, Pennathur S, Kaufman RJ. Chop deletion reduces oxidative stress, improves beta cell function, and promotes cell survival in multiple mouse models of diabetes. *J Clin Invest.* 2008;118(10):3378-3389.
28. Ricci JE, Muñoz-Pinedo C, Fitzgerald P, et al. Disruption of mitochondrial function during apoptosis is mediated by caspase cleavage of the p75 subunit of complex I of the electron transport chain. *Cell.* 2004;117(6):773-786.
29. Korbecki J, Kojder K, Simińska D, et al. CC chemokines in a tumor: a review of pro-cancer and anti-cancer properties of the ligands of receptors CCR1, CCR2, CCR3, and CCR4. *Int J Mol Sci.* 2020;21(21):8412.
30. Li D, Ji H, Niu X, et al. Tumor-associated macrophages secrete CC-chemokine ligand 2 and induce tamoxifen resistance by activating PI3K/Akt/mTOR in breast cancer. *Cancer Sci.* 2020;111(1):47-48.
31. Xue, J., Ge, X., Zhao, W., Xue L., Dai C., Lin F., Peng W. PIPK $\gamma$  regulates CCL2 expression in colorectal cancer by activating AKT-STAT3 signaling. *J Immunol Res* 2019; 2019: 3690561, 12
32. Natsagdorj A, Izumi K, Hiratsuka K, et al. CCL2 induces resistance to the antiproliferative effect of cabazitaxel in prostate cancer cells. *Cancer Sci.* 2019;110(1):279-288.
33. von Roemeling CA, Marlow LA, Wei JJ, et al. Stearoyl-CoA desaturase 1 is a novel molecular therapeutic target for clear cell renal cell carcinoma. *Clin Cancer Res.* 2013;19(9):2368-2380.
34. Xu H, Li S, Sun Y, et al. ELOVL5-mediated long chain fatty acid elongation contributes to enzalutamide resistance of prostate cancer. *Cancer.* 2021;13(16):3957.
35. Centenera MM, Scott JS, Machiels J, et al. ELOVL5 is a critical and targetable fatty acid Elongase in prostate cancer. *Cancer Res.* 2021;81(7):1704-1718.
36. Azrad M, Turgeon C, Demark-Wahnefried W. Current evidence linking polyunsaturated fatty acids with cancer risk and progression. *Front Oncol.* 2013;3:224.
37. Borin TF, Angara K, Rashid MH, Achyut BR, Arbab AS. Arachidonic acid metabolite as a novel therapeutic target in breast cancer metastasis. *Int J Mol Sci.* 2017;18(12):2661.
38. Matsuyama M, Yoshimura R. Relationship between arachidonic acid pathway and human renal cell carcinoma. *Onco Targets Ther.* 2008;1:41-48.
39. Wang D, Dubois RN. Eicosanoids and cancer. *Nat Rev Cancer.* 2010;10(3):181-193.
40. D'Eliseo D, Velotti F. Omega-3 fatty acids and cancer cell cytotoxicity: implications for multi-targeted cancer therapy. *J Clin Med.* 2016;5(2):15.
41. Murray M, Hraiki A, Bebawy M, Pazderka C, Rawling T. Anti-tumor activities of lipids and lipid analogues and their development as potential anticancer drugs. *Pharmacol Ther.* 2015;150:109-128.
42. Yang Q, Wang Y, Yang Q, et al. Cuprous oxide nanoparticles trigger ER stress-induced apoptosis by regulating copper trafficking and overcoming resistance to sunitinib therapy in renal cancer. *Biomaterials.* 2017;146:72-85.
43. Hu H, Tian M, Ding C, Yu S. The C/EBP homologous protein (CHOP) transcription factor functions in endoplasmic reticulum stress-induced apoptosis and microbial infection. *Front Immunol.* 2018;9:3083.
44. Wang Z, Xie H, Zhou L, et al. CCL2/CCR2 axis is associated with postoperative survival and recurrence of patients with non-metastatic clear-cell renal cell carcinoma. *Oncotarget.* 2016;7(32):51525-51534.
45. Arakaki R, Yamasaki T, Kanno T, et al. CCL2 as a potential therapeutic target for clear cell renal cell carcinoma. *Cancer Med.* 2016;5(10):2920-2933.
46. Hoxhaj G, Manning BD. The PI3K-AKT network at the interface of oncogenic signalling and cancer metabolism. *Nat Rev Cancer.* 2020;20(2):74-88.
47. Song M, Bode AM, Dong Z, Lee MH. AKT as a therapeutic target for cancer. *Cancer Res.* 2019;79(6):1019-1031.
48. Martorana F, Motta G, Pavone G, et al. AKT inhibitors: new weapons in the fight against breast cancer? *Front Pharmacol.* 2021;12:662232.
49. Epand RM. Features of the phosphatidylinositol cycle and its role in signal transduction. *J Membr Biol.* 2017;250(4):353-366.
50. Scaglia N, Igal RA. Inhibition of stearyl-CoA desaturase 1 expression in human lung adenocarcinoma cells impairs tumorigenesis. *Int J Oncol.* 2008;33(4):839-850.
51. Rueda-Rincon N, Bloch K, Derua R, et al. p53 attenuates AKT signaling by modulating membrane phospholipid composition. *Oncotarget.* 2015;6(25):21240-21254.

## SUPPORTING INFORMATION

Additional supporting information may be found in the online version of the article at the publisher's website.

**How to cite this article:** Nitta S, Kandori S, Tanaka K, et al. ELOVL5-mediated fatty acid elongation promotes cellular proliferation and invasion in renal cell carcinoma. *Cancer Sci.* 2022;113:2738-2752. doi: [10.1111/cas.15454](https://doi.org/10.1111/cas.15454)